Hindawi
Shock and Vibration
Volume 2018, Article ID 9476146, 16 pages
https://doi.org/10.1155/2018/9476146

Research Article

Effect of Environmental Conditions on the Modal Response of a 10-Story Reinforced Concrete Tower

Marco Regni,[1] **Davide Arezzo**,[1] **Sandro Carbonari**,[1] **Fabrizio Gara**,[1] **and Daniele Zonta**[2]

[1]*Department of Civil and Building Engineering, and Architecture, DICEA, Università Politecnica delle Marche, 60131, Italy*
[2]*Department of Civil and Environmental Engineering, University of Strathclyde, G1 1XQ, UK*

Correspondence should be addressed to Fabrizio Gara; f.gara@univpm.it

Received 2 March 2018; Revised 28 May 2018; Accepted 30 May 2018; Published 5 July 2018

Academic Editor: Emanuele Reccia

We analyse the effect of temperature and wind velocity on the natural frequencies and modal damping ratios of the Faculty of Engineering Tower at the Università Politecnica delle Marche, a 10-story reinforced concrete frame building, permanently monitored with low-noise accelerometers. The data recorded over the first 5 months of monitoring demonstrate that temperature variations and wind intensity have a clear effect on the first three natural frequencies and the corresponding damping ratios. Temperature is positively correlated to the first and second frequencies, corresponding to shear displacement modes and negatively correlated to the third frequency, corresponding to a torsional mode. All frequencies are positively correlated to wind velocity and changes in damping ratios are inversely correlated to any change in frequency. A mechanical explanation of these phenomena is offered, based on a critical review of literature case studies. These results suggest that using changes in modal parameters for damage detection always requires accurate knowledge of the correlation between modal parameters and environmental quantities (temperature, humidity, and wind velocity), an information which is only available through long-term continuous monitoring of the structural response.

1. Introduction

Vibration-based Structural Health Monitoring (SHM) refers to a family of methods pretending to gain information on the damage state of a structure through measurement and analysis of its vibration response. The key idea behind these methods is based on the assumption that a damage alters locally the stiffness, the mass, or the energy dissipation mechanisms of a structural member, which in turn affect the overall structural dynamic behaviour. While in principle this rationale is flawless, its practical application has some limits [1]. First, even the most severe damage may have a limited effect on the global dynamic response of the structure (in other words, the global response may be insensitive to local damage). Second, different damage states may similarly affect the global response, thus inferring the damage based on the observed response is logically an indeterminate problem, unless we make proper assumptions *a priori*. Third, while it is generally true that a structural damage produces changes in the dynamic response, it is not true that any change in the dynamic response is the result of a damage: notably, environmental conditions may produce variations of modal parameters in the same order of those induced by damage and often much bigger.

Vibration-based structural damage detection of civil structures dates back to the early 1980s, as documented by extensive technical literature reviews [2–4]. These early studies include development of methods for optimal sensor placement, selection of the most sensitive parameters to damage, and the definition of techniques to separate changes in the dynamic properties caused by damage from those due to environmental and operational conditions [3]. Interestingly, all these issues are still of strong interest among researchers, as evident in numerous recent works; see for instance [5–7]. Particularly, the use of changes in natural frequency as suitable damage indicators is still a matter of lively discussion. On one side, frequencies, contrary to mode shapes or damping ratios, are easily identified with

a good accuracy even from ambient vibration tests (AVT). The recent improvement and diffusion of effective automated operational modal analysis (OMA) techniques [8–13] have further contributed to elect frequencies as privileged damage detection parameter. On the other hand, natural frequencies are often not especially sensitive to local damage, while they are strongly affected by environmental and operational conditions, such as temperature, humidity [5, 14], and, particularly in the case of tall structures, wind intensity [15].

Separating the effect of damage from the effect of the environment requires the use of statistical models, such as the multiple data regression (MDR) and the Principal Component Analysis (PCA) [16–19], and other suitable compensation techniques [16, 20, 21]. Among the various environmental factors, temperature is especially important: numerous case studies reported in the literature show that natural temperature variations could produce changes in the modal properties much bigger than those induced by a typical structural damage [22] or the normal operational loads [23]. While it is generally understood that temperature affects the natural frequencies of a structure, this relationship is apparently dependent on the particular structure and can be either direct (i.e., frequencies grow with temperature) or inverse (i.e., frequencies decrease with temperature) [24]. Literature cases include bridges, buildings, and heritage structures.

With reference to bridges, Cornwell et al. [25] studied the variability of modal frequencies with temperature of a single span of a bridge concluding that, for the tested structure, modal frequencies can vary significantly (up to 6%) as a consequence of the temperature daily changes. The authors correlated the frequency changes to the temperature differential across the deck. Cross et al. [26] discussed the effects of temperature on the natural frequencies of the Tamar Suspension Bridge in southwest England, concluding that seasonal effects, rather than daily, can be of significance. Analysing the Seohea Grand cable-stayed bridge in South Korea, Kim et al. [27] proposed a systematic procedure to account for environmental conditions changes in the observed structural response, including the elimination of effects due to temperature changes. They found that temperature increments lead to a reduction in the fundamental frequency of the bridge. Jung et al. [28] presented a correlation analysis between the temperature and the fundamental natural frequency of a suspension bridge, showing that the relationship between temperature and natural frequencies is inversely proportional. Zolghadri et al. [29] published a report addressing results of their studies, focused on the effects of temperature on vibrational characteristics of three continuously monitored bridges and a lab specimen. Bridges include a pre-cast I-girder concrete bridge located in Perry, Utah, a concrete box-girder bridge in Sacramento, California, and a steel plate girder bridge in Salt Lake City, Utah, while the lab specimen is a 72-inch long steel plate instrumented with sensors and subjected to temperature changes. While the dynamic properties of the lab specimen showed a very slightly dependence on temperature, real monitored bridges showed clear increasing or decreasing trends of the natural frequencies, depending on modes, with the temperature increase. Jin et al. [30] proposed a new damage detection method, using artificial neural network and an extended Kalman filter, for damage identification in a composite steel girder bridge under severe temperature changes, also considering freezing effects. They found that the natural frequencies decrease when temperature increases, and vice versa.

The effect of the environmental conditions on the natural frequencies is also typically observed in buildings. With reference to a monitored 17-story steel frame building, Nayeri et al. [31] observed a strong correlation between the modal frequency variations and the temperature variations in a 24 h period. Yuen and Kuok [32] examined the fundamental frequencies of a 22-story reinforced concrete building obtained from a one-year monitoring, finding that, contrarily to their numerical estimations, the first three frequencies increased with an increase in ambient temperature. Faravelli et al. [33] analysed the daily fluctuations of frequencies of the Guangzhou New TV Tower (600 m high) in China observing that also ambient temperature variations of few degree Celsius may induce variations in the structural frequencies, up to 0.5%. Mikael et al. [34] focused on the long-term variation of frequency and damping ratios in several buildings and reported contrasting behaviours, including direct and inverse correlation with temperature variations. More recently, Wu et al. [35] presented results of the continuous dynamic monitoring of an office building using ambient vibration measurements in conjunction with a recently developed stochastic subspace identification methodology. The results are examined to recognize effects of environmental conditions: they found that first fundamental frequencies are directly related to the wind speed and indirectly related to the air temperature. Furthermore, the authors identified clear relationships between the root mean square of acceleration and the modal parameters.

Vibration-based SHM has been extensively applied to cultural heritage buildings (e.g., [36–40]). However, a limited number of works focus on the effects of environmental variations on the fundamental frequencies of historic masonry towers. Among the others, Saisi et al. [41] monitored the Gabbia Tower in Mantua and observed an almost linear increase of the fundamental frequencies with the temperature increment. They attributed this phenomenon to the thermal expansion of materials, which produces an overall closing of superficial cracks, minor masonry discontinuities, or mortar gaps. Ramos et al. [39] observed a similar phenomenon in masonry structures and highlighted the significant contribution of humidity. Ubertini et al. [14] investigated the effects of changes in the environmental conditions on the natural frequencies of a monumental masonry bell Tower demonstrating that temperature, rather than humidity, can affect the measured frequencies. The authors found an increase in frequencies of the bending modes with temperature, consistently with mechanism suggested by Saisi et al. [41]. On the other side, they observed a decrement in the frequency of the first torsional mode, and they attributed this behaviour to the slackening induced by temperature of the tie elements and of the fibre reinforcements.

In summary, there is abundancy of evidence in the technical literature that environmental conditions, and particularly temperature, affect the natural frequencies of civil structures,

(a) (b) (c)

Figure 1: View of the Tower: (a) from North-West; (b) from South (c) aerial view from Bing Maps.

including bridges, building, and heritage structures. The correlation between environmental quantity (temperature, humidity, or wind intensity) and frequency can be either direct or inverse, depending on the particular structure and vibration mode, and the way that the two correlate is not easily predictable. Similarly, there is no unanimous agreement on the mechanisms whereby the environmental conditions produce the observed frequency changes.

In this paper, we wish to offer our contribution to the discussion of this subject, by analysing in detail the effect of temperature variations and wind intensity on the modal parameters of a 10-story reinforced concrete building. The case study is the Tower of the Faculty of Engineering at the Università Politecnica delle Marche (UnivPM), in Ancona, Italy. The Tower has been chosen as case study within a research project funded by the UnivPM addressing on the development of low-cost wireless sensors for the continuous dynamic monitoring of buildings (with applications to the SHM field). To this purpose, a permanent monitoring system, based on traditional wired low-noise accelerometers, has been installed to record the dynamic properties of the Tower and their changes with respect to the wind intensity and temperature variations. These data are used as a benchmark to evaluate in the future the effectiveness of the developing low-cost sensors network. This paper illustrates the results of the monitoring over a first operational period of about 5 months. After a brief description of the structure, the preliminary AVTs performed to characterise the dynamics of the building and to design the continuous dynamic monitoring system are addressed. The monitoring system is then described and the results of measurements are presented and discussed, adopting a multiple data regression to interpret effects of ambient parameters variations on modal properties.

2. The UnivPM Faculty of Engineering Tower

The Tower of the Faculty of Engineering at the Università Politecnica delle Marche (UnivPM) is a 10-story building with interstory height of 5 m. Each floor level is conventionally labelled with the letter q followed by their altitude in meters with respect to the sea level, from $q150$ to $q200$ (Figures 1(a) and 1(b)). The Tower was designed and constructed between 1980 and 1983. The structure has a square plan and is constituted by r.c. spatial frames. Depending on the floor, plan dimensions vary between 18.9 and 19.2 in both directions. The building is flanked by a small r.c. wall structure, separated by a structural joint, hosting the stairway, and elevators (Figure 1(b)). The Tower position in the campus is shown in Figure 1(c). Up to the 5^{th} floor, the Tower is adjacent to other r.c. buildings, characterised by a similar structural scheme and separated by expansion joints. The internal partitions are all made of light panels while perimeter walls are built with prefabricated r.c. panels anchored to the frame beams but disconnected from the columns. Between panels of adjacent floors, aluminium window frames are located (Figures 1(a) and 1(b)). Floor slabs are prefabricated predal panels as well as the roof that is of flat type.

R.c. frames are made of 9 columns, equally spaced of 9 m in the two principal directions (Figure 2(a)). Columns have a square cross section with an indentation (5x20 cm) in the central part and dimensions progressively reduced with the building height (Figure 2(c)). It is worth noting that columns of upper floors are divided into 4 square subcolumns having cross sections of dimension 35x35 cm, connected to each other at mid-height with a small r.c. link. Beams have overall a wide of 90 cm and a height of 65 cm. The structure is founded on piles; in particular, 2x2 pile groups with piles of diameter 1 or 1.2 m, depending on the column, are located beneath each column, excepting one edge column, founded on a 3-pile foundation (Figure 2(b)).

During construction, 240 concrete samples were taken and tested at the Materials and Structures Testing Laboratory of UnivPM. Results of experimental tests revealed that the mean cubic strength of concrete is $R_{ck,p}$ = 28.14 MPa for foundation piles, $R_{ck,f}$ = 43.91 MPa for the floors (i.e., for beams), and $R_{ck,c}$ = 41.62 MPa for the columns. As for reinforcements, rebars FeB44k (corresponding to modern B450C) were used.

3. Preliminary AVTs and System Identification

AVTs have been performed with the aim of evaluating the modal parameters of the structure, namely, natural frequencies, modal shapes, and damping ratios. To this purpose, three

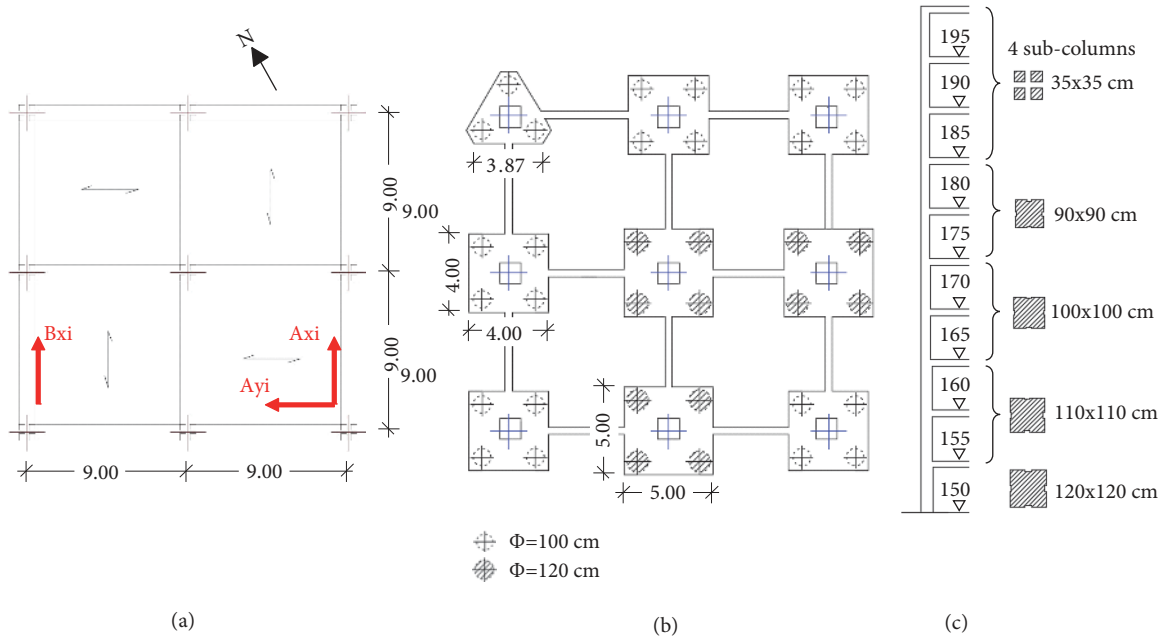

Figure 2: (a) Typical floor plan, (b) foundation layout, and (c) columns cross sections.

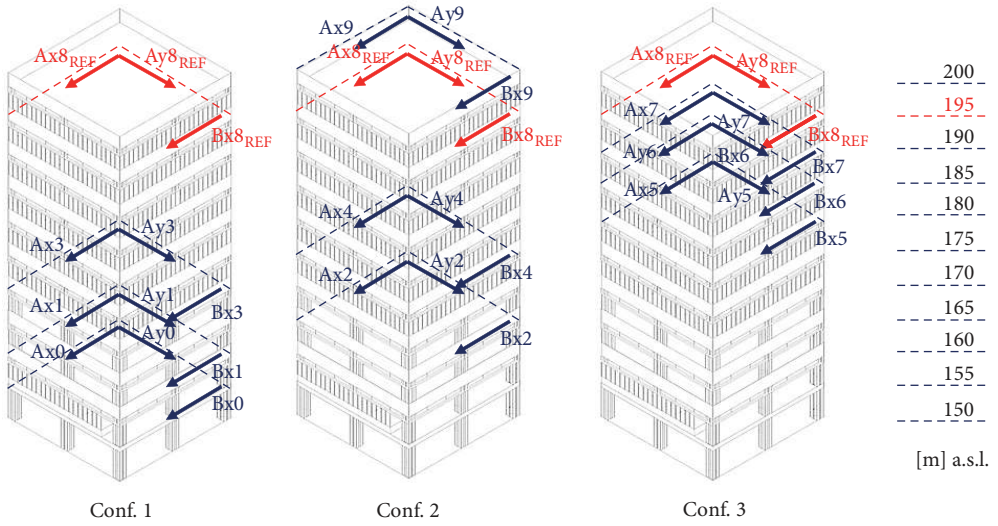

Figure 3: Configurations of AVTs.

piezoelectric monoaxial accelerometers PCB model 393B31 have been placed at each floor to record both translational and rotational components of displacements. Sensors have been connected through coaxial cables to acquisition cards (24-bit NI 9234 acquisition cards and one chassis NI cDAQ-9178) coupled to a laptop and equipped with dedicated software. The position of the sensors on a typical floor is shown in Figure 2(a). Due to the limited number of accelerometers available for the experiment, the measurements have been carried out with three separate sensor configurations, each covering four floors, and always including floor 8 ($q195$) as a reference, as shown in Figure 3. The tests were performed in August 2017.

The fundamental frequency of the structure was preliminary estimated to be around 1 Hz and therefore recordings with a duration of 1800 seconds (30 minutes) were made, dividing each time histories into 90 samples of 20 seconds. The analogic signal is initially recorded at a sampling frequency of 2048 Hz; then, the recorded data are processed with standard signal processing techniques: first a correction of the spurious trends of the signals is performed by using a third-degree polynomial function; then, all the frequency components in the analogic signal above the Nyquist frequency are removed through a low-pass filter with cut-off frequency of 20 Hz to eliminate the contribution of high frequencies and avoid aliasing phenomena; finally, signals were downsampled

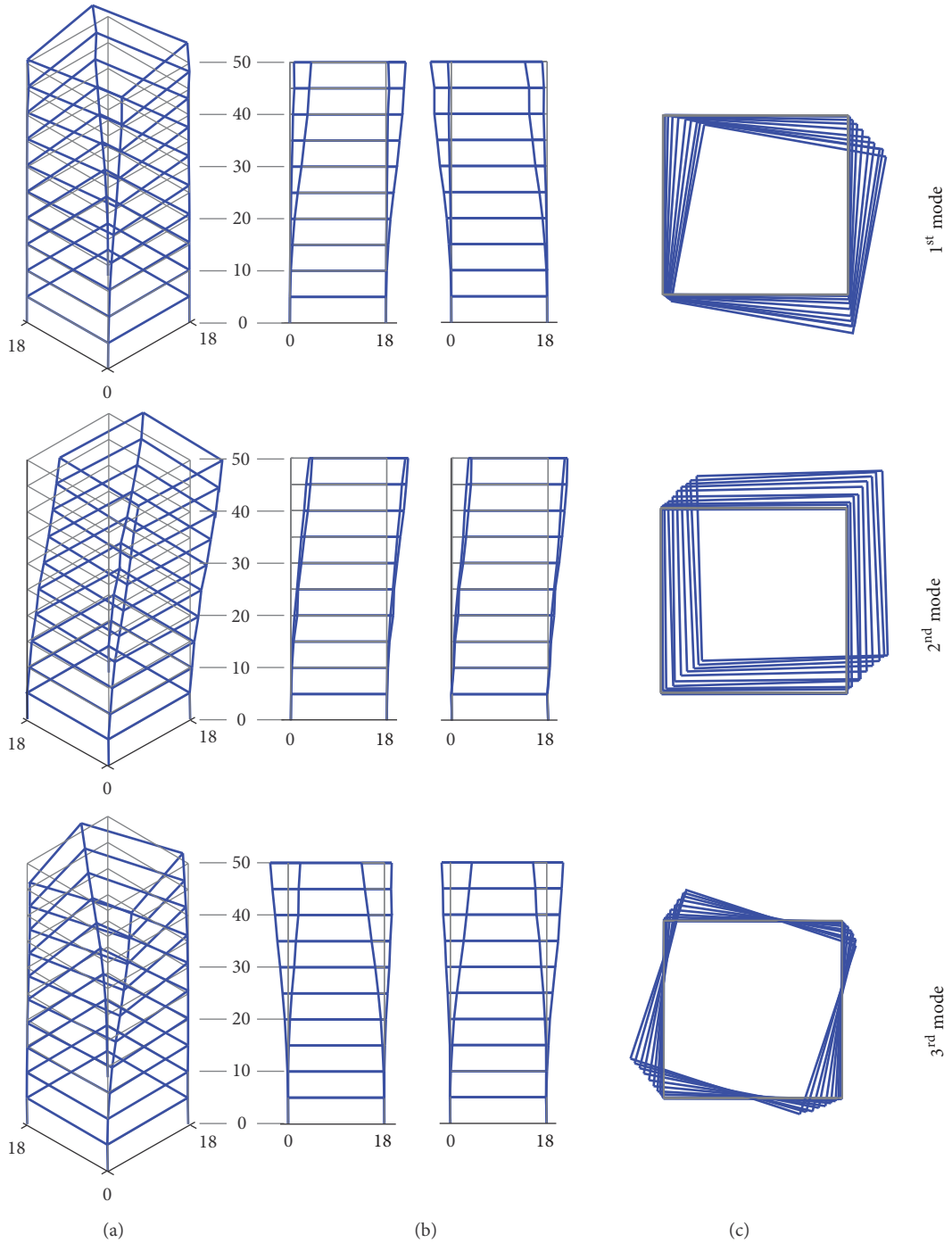

Figure 4: First three global mode shapes of the Tower from AVTs: (a) axonometric view; (b) lateral views; (c) plan view.

at 51.2 Hz to limit the amount of data to be managed. The covariance-driven stochastic subspace identification (SSI-cov) technique [42] was used to identify the dynamic properties of the Tower from the recordings. As stated above, tests were made at different times, according to 3 different sensors configurations; in operational modal analysis of large structures this often occurs, making necessary to process data from multiple nonsimultaneously recorded measurement setups. The Post Separate Estimation Re-scaling (PoSER) approach [43] is used to process data from nonsimultaneous acquisitions. The first three global mode shapes are shown in Figure 4 and the related eigenfrequencies and damping ratios are reported in Table 1.

Results of ambient vibration tests are interpreted through a Finite Element Model (FEM) of the Tower, developed by means of the SAP2000 code [44]. Both beams and columns are modelled with elastic frame elements, while shell elements are used to simulate the floor slabs. The hypothesis of fixed

Table 1: Numerical and experimental first three eigenfrequencies and damping ratios.

Mode	AVTs		3D FEM	Error
	Frequency [Hz]	Damping ratio [%]	Frequency [Hz]	[%]
1st	1.07	2.55	1.15	7.5
2nd	1.21	1.62	1.17	3.3
3rd	1.51	1.86	1.51	0.0

base is assumed, supported by the deep foundations. To better reproduce the building response subjected to small vibrations, nonstructural members (i.e., prefabricated perimeter panels) are included in the model through shell elements (Figure 5(a)). The mechanical properties of the structural concrete are based on the experimental results, conducted in the framework of a recent seismic vulnerability assessment of the building. In particular, 2 cylindrical specimens of diameter $d = 93$ mm and height $h = 93$ mm have been extracted from 2 columns of the Tower (at $q175$ and $q195$, respectively) and 20 pull-out tests were performed on columns (2 tests per floor). Specimens were subjected to compressive tests and results used to calibrate a regression formula to interpret results of pull-out tests. The mechanical characterisation of concrete leads to a mean Young's modulus $E_{cm} = 32493$ MPa, obtained from concrete compressive strength according to [45]. The static value of Young's modulus has been incremented of about 20%, according to suggestions of Lydon et al. [46]. The Tower is separated from adjacent buildings by efficient expansion structural joints; however, continuous nonstructural components may affect sensibly the Tower dynamics and the interpretation of AVTs through the numerical 3D FEM requires adjacent buildings to be modelled. In detail, the r.c. wall structure hosting the stairway and interacting with the Tower for the whole length is included in the model (Figures 5(a) and 5(b)) and connected to the Tower by elastic links, while interactions with lower buildings are taken into account through concentrated compliant restraints (Figure 5(c)). The comparison between the first three numerical (red lines) and experimental mode shapes (blue lines) are reported in Figures 6(a) and 6(b), adopting both an axonometric projection and a plan view of the last floor.

The Tower interaction with the adjacent stairway determine a coupling of the horizontal and torsional modes; numerical results refer to a calibrated model, obtained by updating stiffnesses of elastic links simulating interactions with the stairway, determined by nonstructural components. On the contrary, interactions with lower buildings are of less significance and results shown in Figure 6, which demonstrate a good agreement between numerical and experimental mode shapes, refer to a model disregarding their contributions. The first three natural frequencies obtained with the numerical model are reported in Table 1; differences between numerical and experimental data are of about 7% and 3% for the first and second frequency, respectively, while the third frequency is almost perfectly reproduced.

Comparison between numerical and experimental mode shapes is also presented through the Modal Assurance Criterion (MAC) in Figure 6(c). According to this criterion, a MAC equal to 1 identifies the perfect matching of the experimental and numerical mode shapes while a MAC equal to 0 denotes the orthogonality of the two modes. It is worth noting that the developed model is able to well reproduce the experimental data, in terms of both frequencies and mode shapes.

4. The Continuous Dynamic Monitoring System

According to the cantilever-type behaviour of the system, a simple dynamic monitoring system has been developed, starting on results of AVTs that provides expected frequencies and damping ratios of the first modes. In particular, 3 sensors have been installed at the last floor of the Tower ($q195$), according to layout of Figure 2(a). The system is completely wired and consists of three accelerometers PCB model 393B31 (Figures 7(a) and 7(b)), one data acquisition unit (DAQ), and one PC (Figure 7(c)). The computer can be accessed remotely, in order to download the recorded data and check for any malfunctions. 30-minute samples are acquired twice a day, with registrations beginning at 01:00 and at 13:00 o'clock each day. In addition, 12 samples within 24 hours are acquired one day per month, in order to detect eventual daily wander of modal properties. Values of the air temperature are recorded by a thermometer positioned on the Tower and protected from the solar exposure. The mean internal temperature is regulated by a centralised conditioning system and very moderate daily changes have been observed, during one week long monitoring through a portable thermometer. Mean temperatures of 19°C and 25°C have been observed during the summer and winter periods, respectively. The wind velocity is obtained by two weather stations very close to the Engineering Faculty, the Brecce Bianche, and the Q2 weather stations. Position of the two stations with respect to the Engineering faculty of the Università Politecnica delle Marche are shown in Figure 7(d). The continuous dynamic monitoring system was installed on the Tower in August 2017 and it is still fully operative.

The acquisition software has been *ad hoc* developed in Labview, a system-design platform and development environment for a visual programming language from National Instruments [47]. The analogic signal is sampled at 2048 Hz and resampled at 51.2 Hz before the storage. To avoid aliasing, all the frequency components in the analogic signal that are above the Nyquist frequency are removed through a low-pass filter and then eventual offset is eliminated. An automated procedure was developed within the acquisition algorithm to extract the desired modal parameters exploiting the SSI-based toolkit proposed by Hu et al. [48]. The procedure

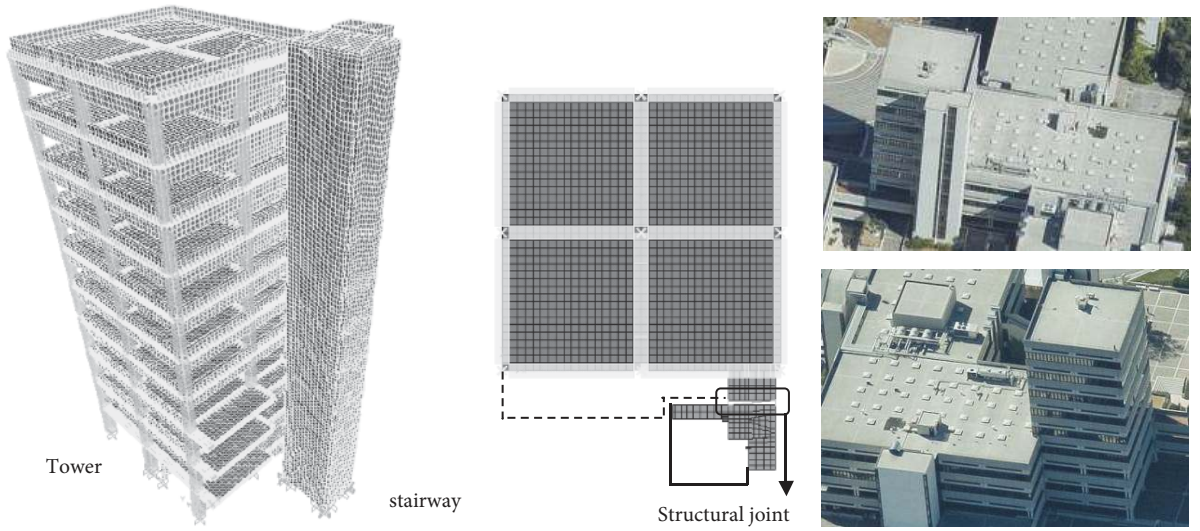

Figure 5: (a) 3D finite element model of the Tower; (b) plan view of the floor slab; (c) Tower interactions with adjacent buildings.

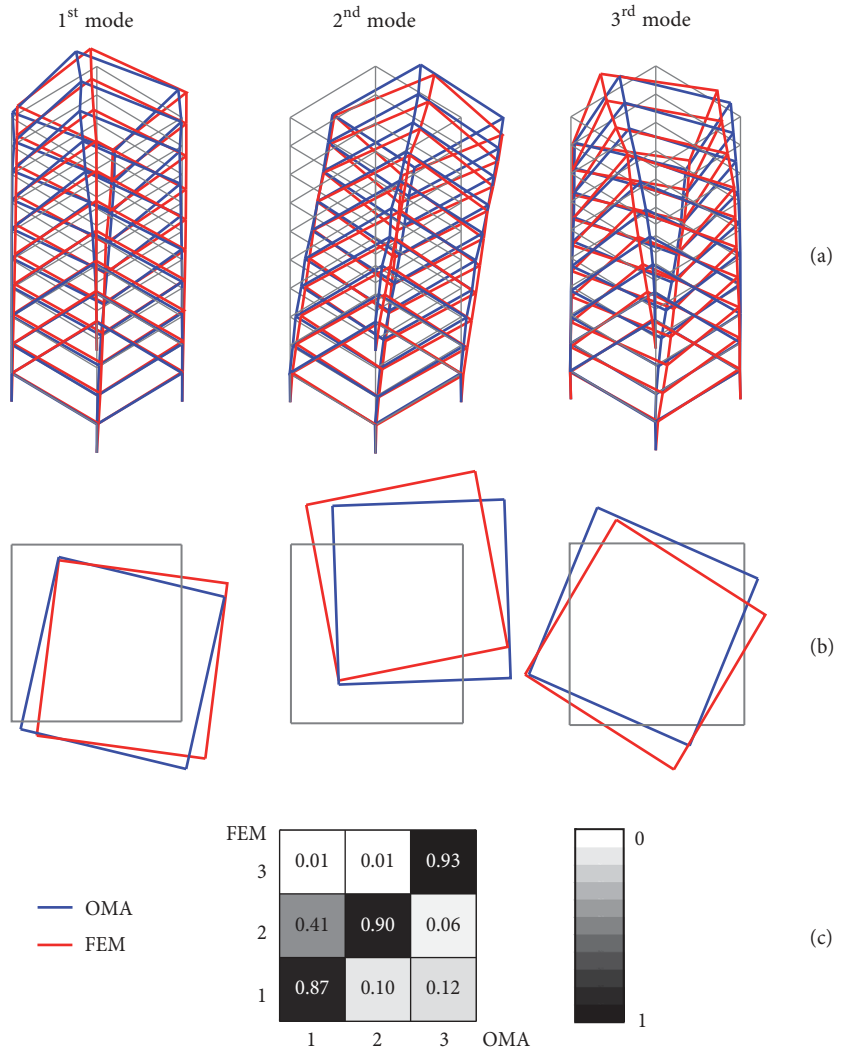

Figure 6: Comparison of experimental and numerical mode shapes: (a) axonometric view; (b) plan view of the last floor; (c) MAC.

Figure 7: (a) Accelerometer at position Bx; (b) accelerometers at positions Ax and Ay; (c) acquisition station.

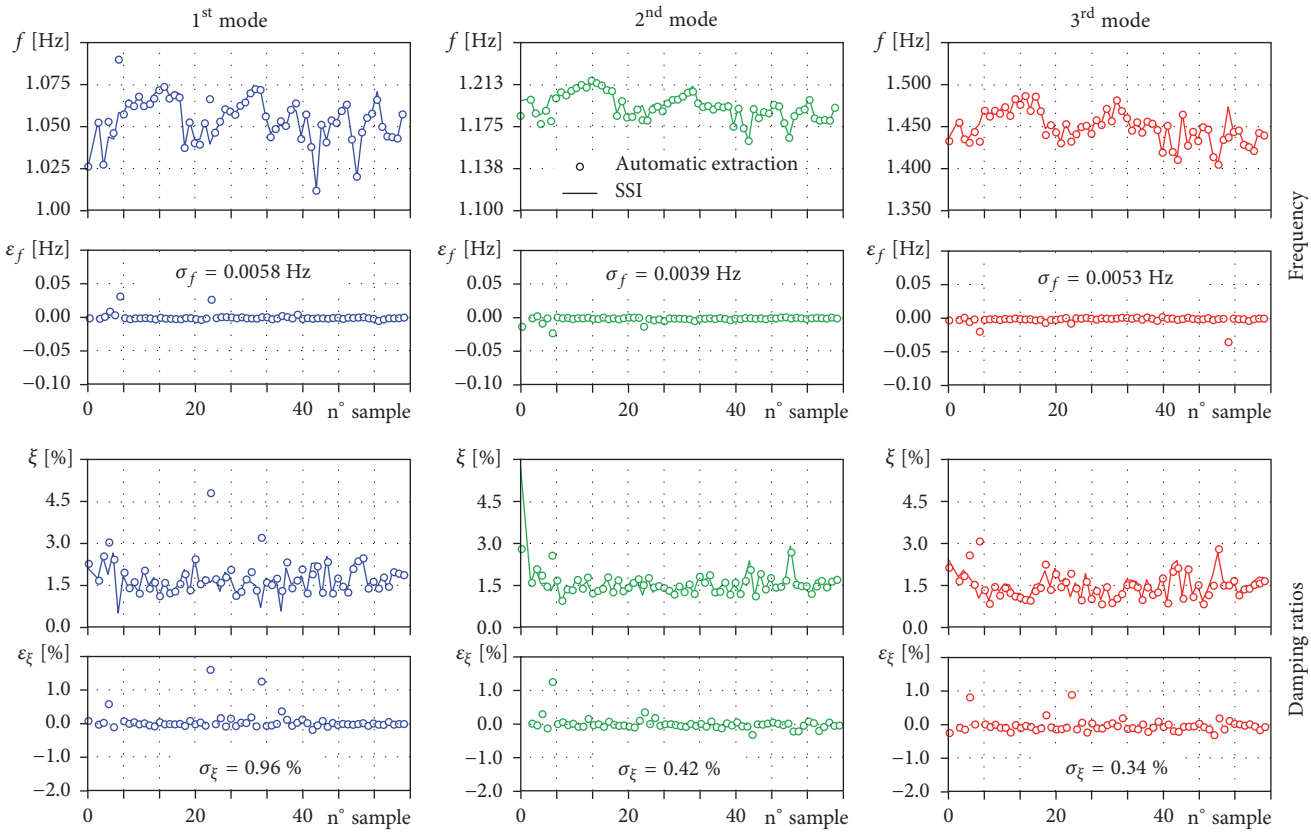

Figure 8: Comparison of modal parameters extracted from the automated procedure and from the SSI approach; (b) errors of the developed algorithm.

allows handling the daily vibration measurements and the acquisitions of the air temperature and the wind velocity; the latter is obtained through the weathers stations websites. Furthermore, the algorithm assures the data storage on a dedicated server for future in-depth analysis. Figure 8 compares results obtained from the developed automated procedure and a robust consolidated algorithm, based on the SSI approach [42], over a period of 1 month (i.e., 60 samples). In particular, fundamental frequencies and damping ratios of the first three vibration modes automatically obtained (dots) are compared with the relevant values resulting from the SSI analysis (continuous lines) performed on the stored data. For each mode, Figure 8 also shows residuals ε_i ($i = f, \xi$) between the two approaches and the standard deviation σ_i of the residuals distribution. Residuals relevant to natural frequencies are very low (the error of the automatic extracted

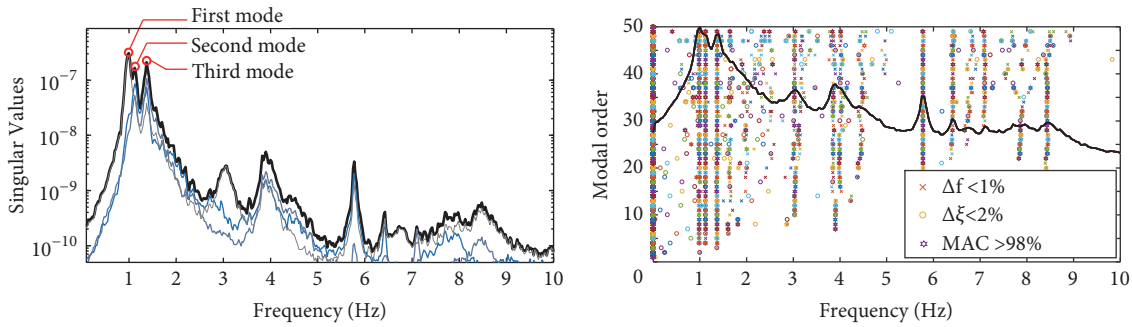

Figure 9: (a) Singular-Value Decomposition plot and (b) typical stabilization diagram of an acquisition.

values are below 0.5% for the majority of samples and all modes) while residuals of modal damping ratios are sensibly higher, with a mean error of about 30%.

Figures 9(a) and 9(b) show the Singular-Value Decomposition (SVD) of a typical record for the setup of the monitoring system and the stabilization diagram of a typical acquisition, respectively. The SVD plot clearly highlights the first fundamental frequencies of the system while higher modes are less evident, according to the sensors position.

5. Monitoring Outcomes

This section shows results of the Tower monitoring from August 11, 2017, to December 17, 2017. Data from a total of 207 30-minute acquisitions are statistically reelaborated. Figure 10 shows the evolution of the air temperature (T) and wind velocity (w) during the monitoring period. It can be observed that some data in September and October 2017 are missing, due to a temporal shout-down of the acquisition software handling the environmental parameters (grey filled areas). Furthermore, a technical inconvenient also occurred in November 2017, also causing the loss of the vibrational measurements (grey filled area). The acquisition software has been enhanced according to the encountered problems to avoid future measurements breaks. Available environmental data show an evident seasonal and daily variation of temperatures. On the contrary, wind velocities are less governed by seasonal fluctuations, even if the higher values have been registered in relatively cold months (October and December). With reference to wind, daily fluctuations are more pronounced, probably due to the land and sea breezes, typical of coastal areas. The automated identification of the modal frequencies and damping ratios from the dataset resulted in the frequency and damping histories reported in Figure 10. At a first glance, dependency of modal parameters to the wind intensity is evident with the all fundamental frequencies reducing significantly in occasion of registered high wind velocities (grey dashed lines).

Figure 11 shows similar quantities obtained from the daily monitoring of selected days (one per month). Wander in frequencies, even if of minor amplitude, is also visible in the daily frequencies trends shown in Figure 11. In particular, a significant increase of the first frequency can be observed with the temperature increment on 11 August (h 12:00) at almost constant wind velocities. Overall higher frequencies are observed on 12 October with respect to 11 August and 12 September, consistently with the lower values of the wind velocities. Moreover, by assuming that 12 October and 17 November are characterised by the same mean wind velocities, overall higher values of frequencies are observed on October, in correspondence of higher registered temperatures. Finally, an overall increase of the third frequency is observed from August to November, namely, for decreasing air temperatures.

By assuming a normal distribution of the dynamic parameters, statistics of modal parameters are reported in Table 2, which includes the mean values and the standard deviation of fundamental frequencies and modal damping ratios, as well as the relevant Coefficient of Variation (COV). It can be observed that standard deviation values of natural frequencies are very low; on the contrary, standard deviation of damping ratios are sensibly higher; thus, damping ratios are much more dispersed than frequencies, as confirmed by COVs.

Figure 10 shows a sensitive variation of the fundamental frequencies with respect to environmental conditions. In order to better address the phenomenon, each frequency and damping ratio is plotted with respect to the relevant value of temperature and wind velocity.

Figures 12(a) and 12(b) show variations of the identified fundamental frequencies and damping ratios with respect to air temperature and wind velocity, respectively. The best fitting lines, in the least square sense, are shown with black lines. As can be observed from Figure 12(a), although highly scattered, results demonstrate a positive interaction of the first and second frequencies with the temperature while a negative pronounced interaction is observed for the third frequency. Damping ratios are characterised by opposite trends; overall, a decrement of the damping ratio is observed for an increment of the vibration frequency, consistently with the "apparent" stiffness increase and the reduction of the dissipative contributions (e.g., material damping effects, frictions between structural and nonstructural elements, and small nonlinear effects). Concerning dependency of modal parameter on wind velocity, it can be observed from Figure 12(b) that all frequencies decrease by increasing the

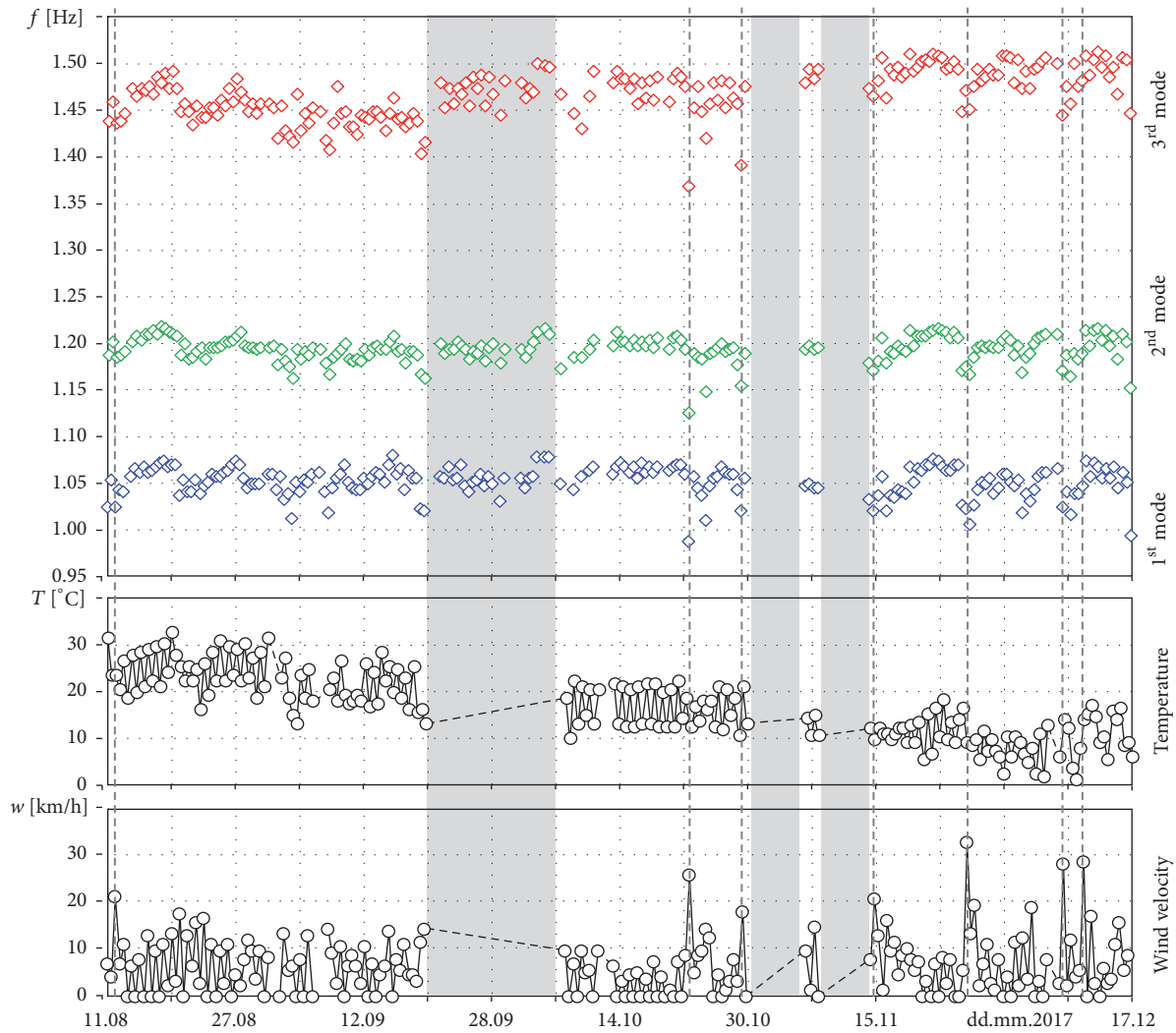

Figure 10: Evolution of the air temperature and wind velocity during the monitoring period and histories of identified fundamental frequencies.

Table 2: Statistics of eigenfrequencies and damping ratios.

Mode	Frequencies			Damping ratios [%]		
	Mean [Hz]	Standard deviation [Hz]	COV [%]	Mean [Hz]	Standard deviation [Hz]	COV
1st	1.0518	0.0159	1.51	1.9625	0.5994	30.54
2nd	1.1931	0.0136	1.14	1.6256	0.4296	26.43
3rd	1.4667	0.0258	1.76	1.6105	0.4822	29.94

wind speed. This can be justified by the increase of the external actions that leads the structure to develop higher small nonlinear effects or frictions between elements.

This hypothesis can be supported by the observation that a decrease in the frequency is always associated with an increase in the value of the damping ratio, as can be observed from Figure 13. The relationship between frequency and damping ratio shown in Figure 13, as well as previous considerations concerning trend of frequencies and damping ratios with respect to the wind velocities, can be better interpreted by observing the variation of the modal parameters with respect to the root mean square (RMS) of the recorded (Figure 14) acceleration signals opportunely filtered with a band-pass filter (in the range 0.5 – 3.0 Hz) in order to eliminate contributions not related to the investigated modes. It can be observed that by increasing the amplitude of the acceleration a reduction of the fundamental frequencies and an increase of the relevant damping ratios are observed. Data are interpolated with power functions and the relevant coefficient of determination is reported in the graph; although few data are characterised by acceleration higher that 45 μg, the regression model, which quite well fits the experimental

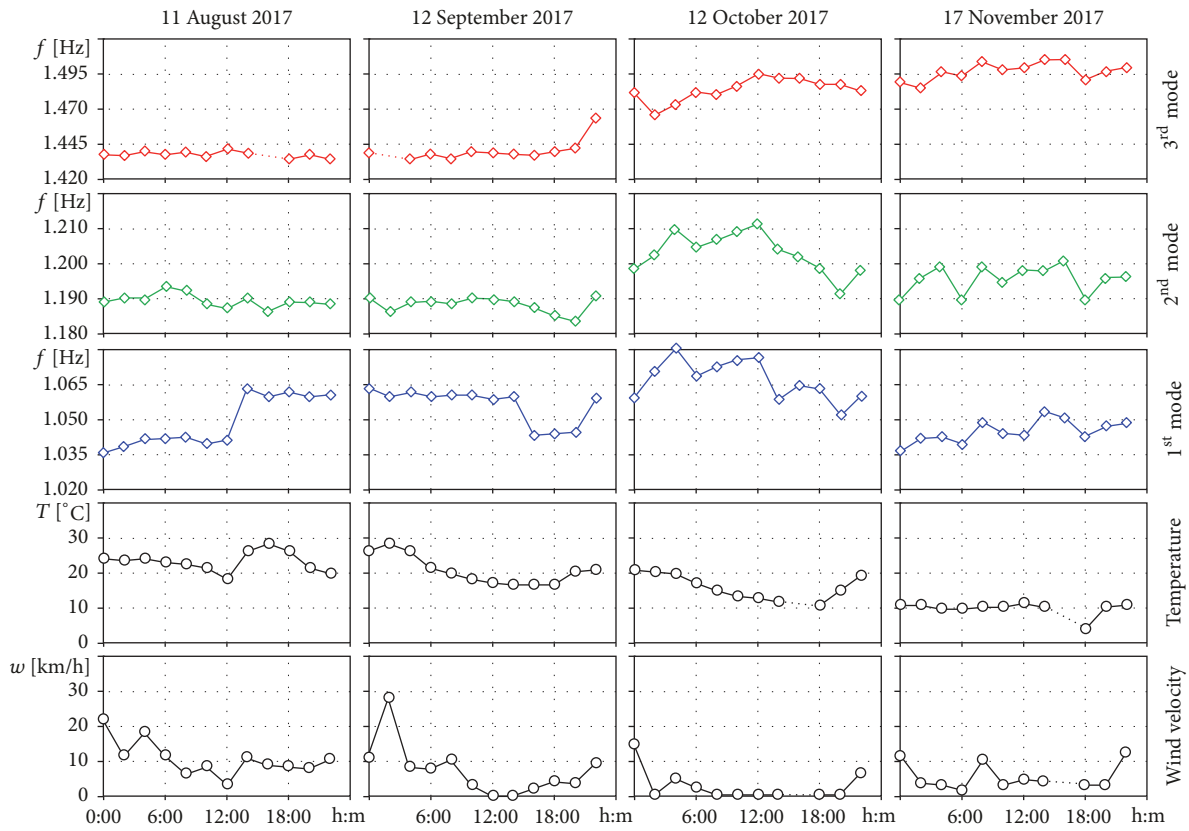

FIGURE 11: Daily evolution of the air temperature and wind velocity for selected days and histories of identified fundamental frequencies.

results, reveals that phenomena inducing the frequencies decrease and damping ratio increase tend to saturate.

This is consistent with the hypothesized nature of these phenomena that, as previously stated, may be due to small frictions developing between structural and nonstructural elements.

Although clear trends of frequencies and damping ratios can be observed due to changes of temperature and wind velocity, it should be remarked that weather phenomena occur simultaneously and effects on the modal parameters are strictly correlated. From a more rigorous point of view, the MDR technique is used to find linear correlations between frequencies and the two independent environmental variables (air temperature and wind velocity). From a formal point of view, and with only reference to frequencies, the regression model is described by

$$\widehat{\mathbf{F}} = \mathbf{AX} \tag{1}$$

where

$$\widehat{\mathbf{F}} = \left[\widehat{f}_1 \quad \widehat{f}_2 \quad \widehat{f}_3\right]^T \tag{2a}$$

$$\mathbf{X} = \left[1 \quad T \quad w\right]^T \tag{2b}$$

are the vectors of estimates of the first three fundamental frequencies $\widehat{f}_1$, $\widehat{f}_2$, and $\widehat{f}_3$ and the vector of the independent environmental variables, respectively. Furthermore, **A** is a 3x3 full matrix of coefficients weighting contributions of environmental parameters for all the fundamental frequencies. Coefficients are determined according to a least square scheme that can be formulated according to

$$\min_{\mathbf{A}} \boldsymbol{g}(\mathbf{A}) = \frac{\mathbf{1}}{\mathbf{2}} \sum_{j=1}^{N} (\mathbf{AX} - \mathbf{F})_j^2 \tag{3}$$

where g is the objective function depending on the unknown parameters **A** and N is the number of the couple of data $(\mathbf{F},\mathbf{X})_j$. **F**, similar to $\widehat{\mathbf{F}}$, is the vector collecting the identified first three fundamental frequencies. It is worth noting that since only two environmental parameters are considered, the regression models (1) correspond to planes. Matrix **A**, obtained from the linear least square optimization, assumes the following form:

$$\mathbf{A} = \begin{bmatrix} 10520 & 6.2997 & -15.787 \\ 11978 & 2.3042 & -12.083 \\ 15014 & -16.143 & -11.645 \end{bmatrix} 10^{-4} \tag{4}$$

Components of matrix **A** reveal positive and negative interactions of frequencies with ambient parameters. It is worth noting that, with reference to the first two frequencies, coefficients of temperature are sensibly lower than those of wind velocity while for the third frequency coefficient of temperature is higher. This implies that frequency variations of the first and second mode are more related to variations of

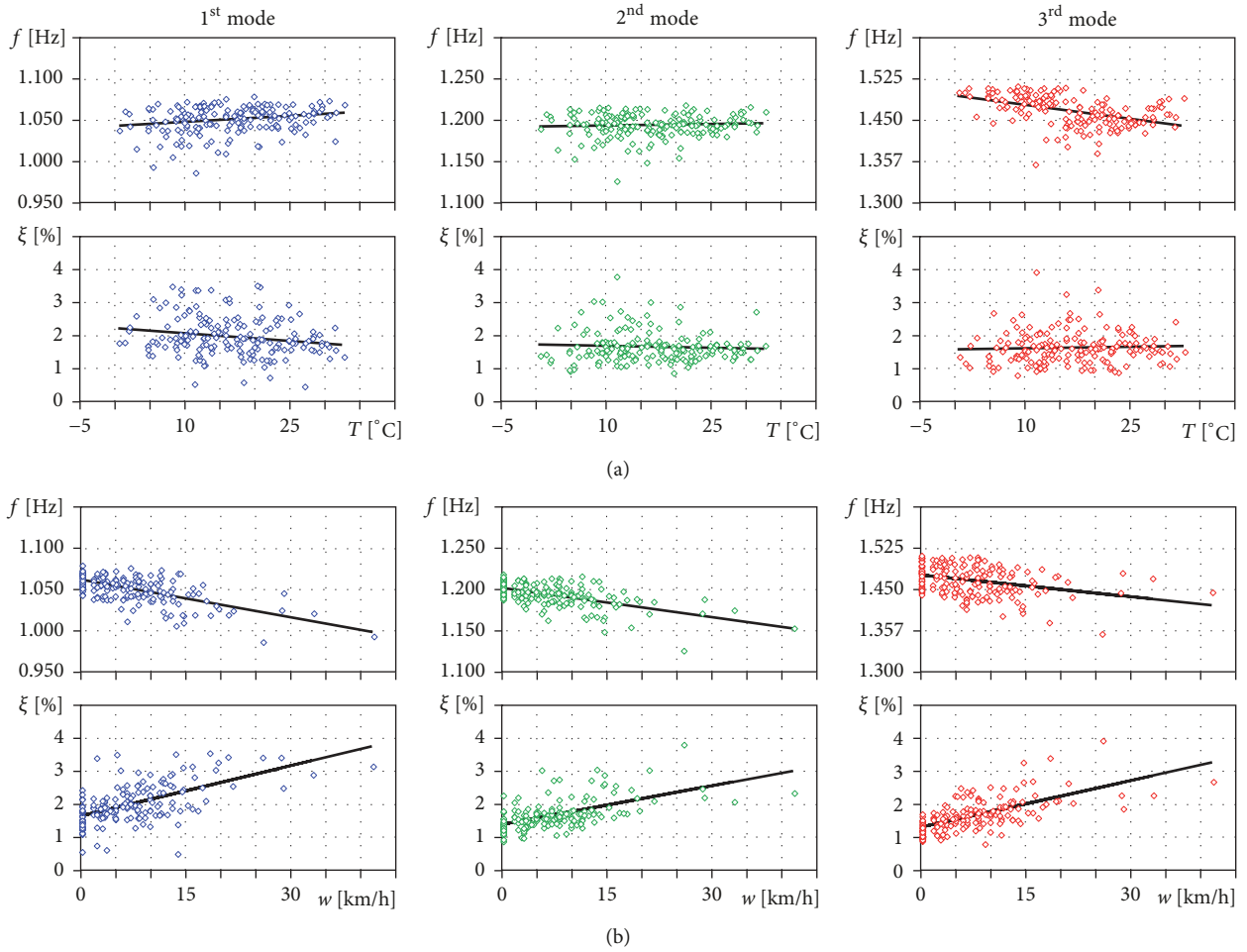

Figure 12: Variation of frequencies and damping ratios: (a) variations with respect to temperature and (b) variations with respect to wind velocity.

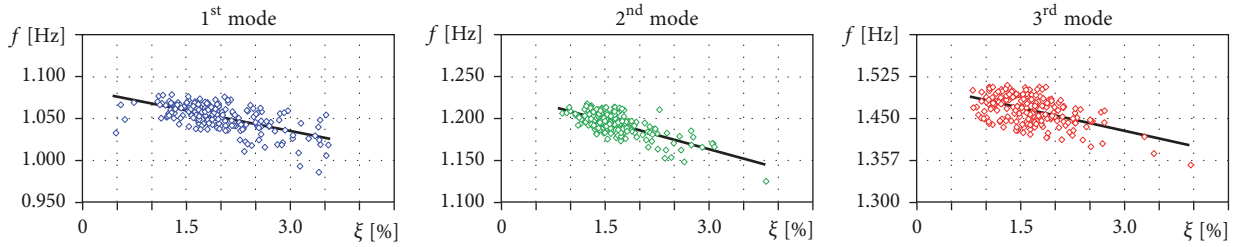

Figure 13: Correlation between frequencies and damping ratios.

the wind velocity than to variations of ambient temperatures while for the third mode frequency variations are almost equally influenced by both ambient parameters.

Figure 15 shows results of the MDR analysis performed with reference to the first three fundamental vibration frequencies. In detail, regression planes are reported and the relevant R-squared coefficients are included to provide an idea of the fitting goodness.

In addition, components of the residual vector (**AX**-**F**) are plotted for all the samples. Trends of frequencies with temperature and wind velocities previously highlighted disregarding the combined effects of the environmental parameters are confirmed by the MDR.

The first and second frequencies show a positive interaction with temperature and a negative interaction with the wind velocity while the third frequency shows a negative interaction with both temperature and wind velocity. As previously observed, the increase of all fundamental frequencies with the increase of the wind velocity may be due to the development of small nonlinear effects or frictions between structural and nonstructural elements, activated by the increasing wind velocity and amplitude of oscillations.

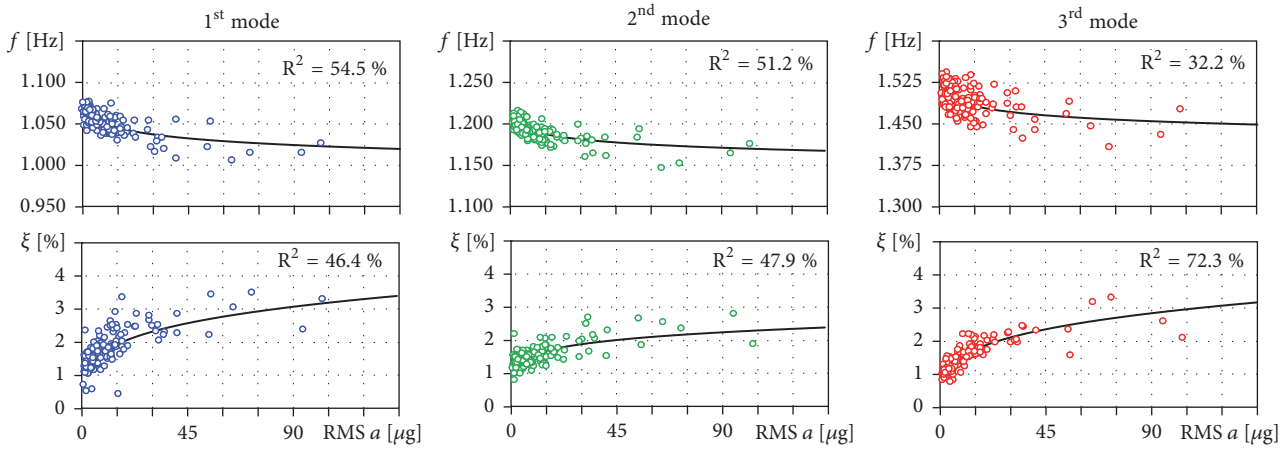

Figure 14: Variation of frequencies and damping ratios with respect to the amplitude of the measured acceleration (RMS).

On the other hand, the contribution of temperature on the fundamental frequencies is more difficult to interpret; trends agree with what observed in the literature concerning the behaviour of a masonry structures [14, 41]; although the structural typology of the presented case study is completely different, considerations concerning the thermal expansion in the material, which may determine an overall closing of microcracks, can hold, leading to an overall increase of the first two fundamental frequencies. Furthermore, thermal expansion, acting on both structural and nonstructural elements, may be responsible for an increase of the coupling between the two components of the building, making the structure overall stiffer.

6. Conclusions

We discussed the effect of temperature variations and wind intensity on the fundamental frequencies and modal damping ratios of the UnivPM Faculty of Engineering Tower, a 10-story r.c. framed building, permanently monitored with low-noise accelerometers. The analysis of the data recorded over the first 5 months of operation of the monitoring system demonstrates that temperature variations and wind intensity have a clear effect on the first three natural frequencies and the corresponding modal damping ratios. In detail,

(i) with respect to temperature, we observed a positive correlation of the first and second frequencies, corresponding to lateral displacement modes, and a sharp negative correlation of the third frequency, corresponding to a torsional mode. The sign of the correlation trends, positive for the first two frequencies and negative for the third, is curiously analogous to those reportedly observed in masonry towers;

(ii) for masonry towers, the increase of the fundamental frequencies is explained with the stiffening of the structure produced by microcracks reclosure in the mortar layers, as a result of thermal expansion. To explain the observed behaviour of the UnivPM building, we can suppose that a similar phenomenon occurs for microcracks in concrete. An alternative explanation, or contributory cause, is that thermal expansion enhances the degree of connection between structural and nonstructural prefabricated elements, eventually increasing the global stiffness;

(iii) with respect to wind, all frequencies decrease by increasing the wind speed. This can be justified by the increase of the external actions that leads the structure to develop higher small nonlinear effects or frictions between structural and nonstructural elements;

(iv) the frequencies associated with bending modes appears more sensitive to the wind velocity rather than to the air temperature, while the frequency of the torsional mode is equally dependent on both environmental factors;

(v) the damping ratios generally decrease by increasing the vibration frequency.

The results presented in this paper demonstrate, once again, that modal parameters are strongly affected by environmental and operational conditions. It is clear that using changes in modal parameters for damage detection always requires proper compensation from the environmental effects. This in turn requires accurate knowledge of the correlation between modal parameters and environmental quantities (temperature, humidity, and wind velocity), an information which is available only after long-term continuous monitoring of the structural behaviour.

Data Availability

The data used to support the findings of this study are available from the corresponding author upon request.

Conflicts of Interest

The authors declare that there are no conflicts of interest regarding the publication of this paper.

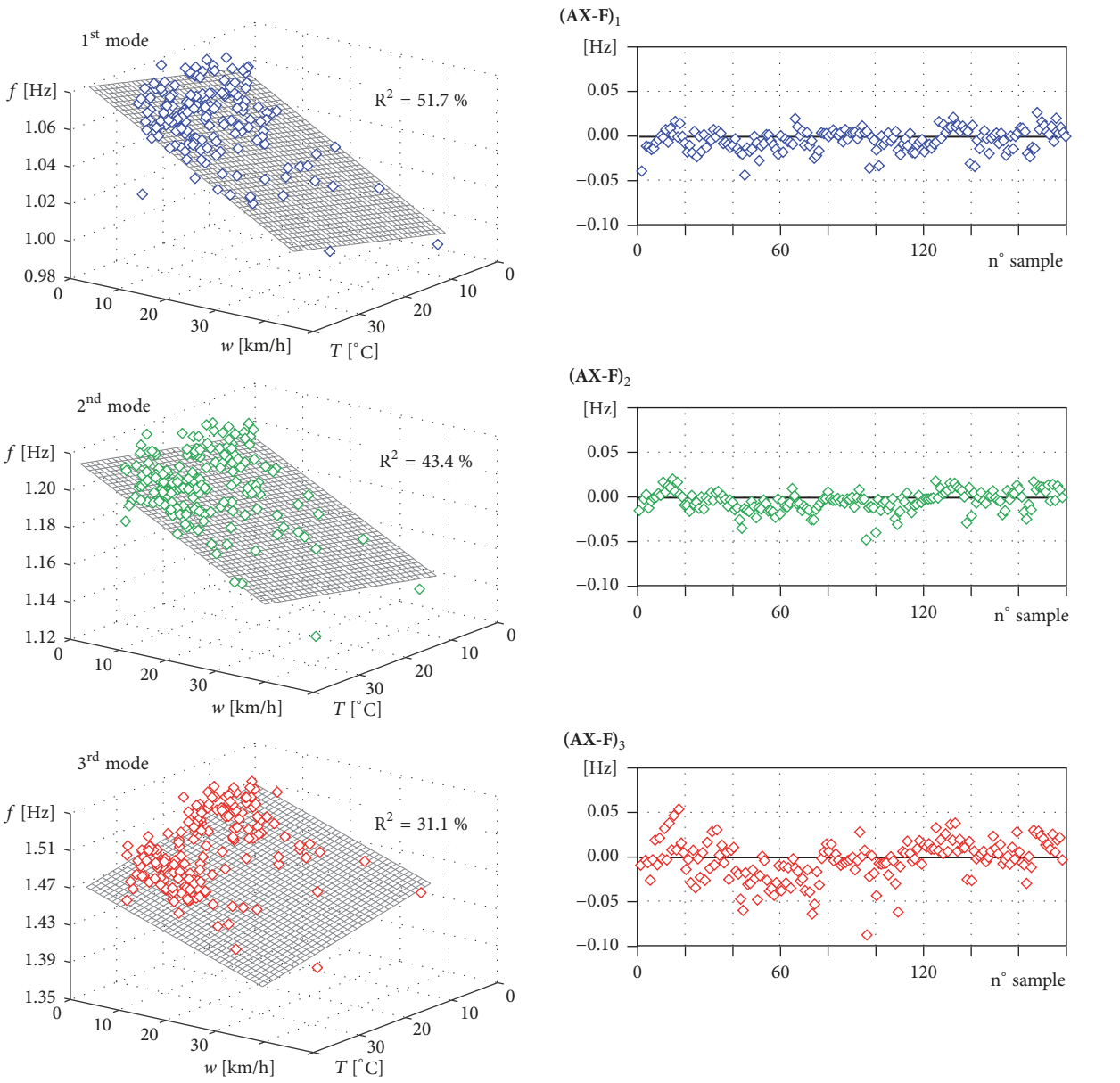

FIGURE 15: Multiple data regression of the first three fundamental frequencies and residuals.

Acknowledgments

This research was supported by the Scientific Research Project 2016 "Structural Health Monitoring of Constructions with Wireless Sensor Network", funded by the Università Politecnica delle Marche.

References

[1] A. Deraemaeker and K. Worden, *New trends in vibration based structural health monitoring*, Springer Wien New York, 2010.

[2] S. W. Doebling, C. R. Farrar, M. B. Prime, and D. W. Shevitz, "Damage identification and health monitoring of structural and mechanical systems from changes in their vibration characteristics: a literature review," Tech. Rep. LA-13070-MS, Los Alamos National Laboratory, 1996.

[3] H. Sohn, "Effects of environmental and operational variability on structural health monitoring," *Philosophical Transactions of the Royal Society A: Mathematical, Physical & Engineering Sciences*, vol. 365, no. 1851, pp. 539–560, 2007.

[4] C. R. Farrar and K. Worden, "An introduction to structural health monitoring," *Philosophical Transactions of the Royal Society A: Mathematical, Physical & Engineering Sciences*, vol. 365, no. 1851, pp. 303–315, 2007.

[5] A. Deraemaeker, E. Reynders, G. De Roeck, and J. Kullaa, "Vibration-based structural health monitoring using output-only measurements under changing environment," *Mechanical Systems and Signal Processing*, vol. 22, no. 1, pp. 34–56, 2008.

[6] A. Alvandi and C. Cremona, "Assessment of vibration-based damage identification techniques," *Journal of Sound and Vibration*, vol. 292, no. 1-2, pp. 179–202, 2006.

[7] A. L. Materazzi and F. Ubertini, "Eigenproperties of suspension bridges with damage," *Journal of Sound and Vibration*, vol. 330, no. 26, pp. 6420–6434, 2011.

[8] F. Magalhães, A. Cunha, and E. Caetano, "Vibration based structural health monitoring of an arch bridge: from automated OMA to damage detection," *Mechanical Systems and Signal Processing*, vol. 28, pp. 212–228, 2012.

[9] F. Magalhães, Á. Cunha, and E. Caetano, "Online automatic identification of the modal parameters of a long span arch bridge," *Mechanical Systems and Signal Processing*, vol. 23, no. 2, pp. 316–329, 2009.

[10] C. Rainieri and G. Fabbrocino, "Automated output-only dynamic identification of civil engineering structures," *Mechanical Systems and Signal Processing*, vol. 24, no. 3, pp. 678–695, 2010.

[11] F. Ubertini, C. Gentile, and A. L. Materazzi, "Automated modal identification in operational conditions and its application to bridges," *Engineering Structures*, vol. 46, pp. 264–278, 2013.

[12] A. Cabboi, F. Magalhães, C. Gentile, and Á. Cunha, "Automated modal identification and tracking: Application to an iron arch bridge," *Structural Control and Health Monitoring*, vol. 24, no. 1, p. e1854, 2017.

[13] R. Cardoso, A. Cury, and F. Barbosa, "A robust methodology for modal parameters estimation applied to SHM," *Mechanical Systems and Signal Processing*, vol. 95, pp. 24–41, 2017.

[14] F. Ubertini, G. Comanducci, N. Cavalagli, A. Laura Pisello, A. Luigi Materazzi, and F. Cotana, "Environmental effects on natural frequencies of the San Pietro bell tower in Perugia, Italy, and their removal for structural performance assessment," *Mechanical Systems and Signal Processing*, vol. 82, pp. 307–322, 2017.

[15] H. Li, S. Li, and J. Ou, "Modal identification of bridges under varying environmental conditions: temperature and wind effects," *Structural Control and Health Monitoring*, vol. 17, no. 5, pp. 495–512, 2010.

[16] K. Worden, H. Sohn, and C. R. Farrar, "Novelty detection in a changing environment: regression and inter polation approaches," *Journal of Sound and Vibration*, vol. 258, no. 4, pp. 741–761, 2002.

[17] A.-M. Yan, G. Kerschen, P. de Boe, and J.-C. Golinval, "Structural damage diagnosis under varying environmental conditions—part I: a linear analysis," *Mechanical Systems and Signal Processing*, vol. 19, no. 4, pp. 847–864, 2005.

[18] A.-M. Yan, G. Kerschen, P. De Boe, and J.-C. Golinval, "Structural damage diagnosis under varying environmental conditions—part II: local PCA for non-linear cases," *Mechanical Systems and Signal Processing*, vol. 19, no. 4, pp. 865–880, 2005.

[19] A. Bellino, A. Fasana, L. Garibaldi, and S. Marchesiello, "PCA-based detection of damage in time-varying systems," *Mechanical Systems and Signal Processing*, vol. 24, no. 7, pp. 2250–2260, 2010.

[20] A. A. Mosavi, D. Dickey, R. Seracino, and S. Rizkalla, "Identifying damage locations under ambient vibrations utilizing vector autoregressive models and Mahalanobis distances," *Mechanical Systems and Signal Processing*, vol. 26, no. 1, pp. 254–267, 2012.

[21] G. Comanducci, F. Ubertini, and A. L. Materazzi, "Structural health monitoring of suspension bridges with features affected by changing wind speed," *Journal of Wind Engineering & Industrial Aerodynamics*, vol. 141, pp. 12–26, 2015.

[22] O. S. Salawu, "Detection of structural damage through changes in frequency: a review," *Engineering Structures*, vol. 19, no. 9, pp. 718–723, 1997.

[23] Y. L. Xu, B. Chen, C. L. Ng, K. Y. Wong, and W. Y. Chan, "Monitoring temperature effect on a long suspension bridge," *Structural Control and Health Monitoring*, vol. 17, no. 6, pp. 632–653, 2010.

[24] Y. Xia, B. Chen, S. Weng, Y.-Q. Ni, and Y.-L. Xu, "Temperature effect on vibration properties of civil structures: a literature review and case studies," *Journal of Civil Structural Health Monitoring*, vol. 2, no. 1, pp. 29–46, 2012.

[25] P. Cornwell, C. R. Farrar, S. W. Doebling, and H. Sohn, "Environmental variability of modal properties," *Experimental Techniques*, vol. 23, no. 6, pp. 45–48, 1999.

[26] E. J. Cross, K. Y. Koo, J. M. W. Brownjohn, and K. Worden, "Long-term monitoring and data analysis of the Tamar Bridge," *Mechanical Systems and Signal Processing*, vol. 35, no. 1-2, pp. 16–34, 2013.

[27] Y. Kim, M. W. Cho, S. Shin, and J. C. Park, "Health monitoring of a cable stayed bridge considering the temperature change," in *Proceedings of the Second Conference on Smart Monitoring, Assessment and Rehabilitation of Civil Structures*, 2013.

[28] J. Jung, D. Moon, J. Jung, S. Ro, and J. Park, "A Correlation Analysis Regarding the Temperature Effect for a Suspension Bridge," *Dynamics of Civil Structures*, vol. 2, pp. 99–106, 2015.

[29] N. Zolghadri, M. W. Halling, P. J. Barr, and N. Foust, "Effects of Temperature on Bridge Dynamic Properties," Final Report CAIT-UTC-050, 2015.

[30] C. Jin, S. Jang, X. Sun, J. Li, and R. Christenson, "Damage detection of a highway bridge under severe temperature changes using extended Kalman filter trained neural network," *Journal of Civil Structural Health Monitoring*, vol. 6, no. 3, pp. 545–560, 2016.

[31] R. D. Nayeri, S. F. Masri, R. G. Ghanem, and R. L. Nigbor, "A novel approach for the structural identification and monitoring of a full-scale 17-story building based on ambient vibration measurements," *Smart Materials and Structures*, vol. 17, no. 2, Article ID 025006, 2008.

[32] K.-V. Yuen and S.-C. Kuok, "Ambient interference in long-term monitoring of buildings," *Engineering Structures*, vol. 32, no. 8, pp. 2379–2386, 2010.

[33] L. Faravelli, F. Ubertini, and C. Fuggini, "System identification of a super high-rise building via a stochastic subspace approach," *Smart Structures and Systems*, vol. 7, no. 2, pp. 133–152, 2011.

[34] A. Mikael, P. Gueguen, P.-Y. Bard, P. Roux, and M. Langlais, "The analysis of long-term frequency and damping wandering in buildings using the Random decrement Technique," *Bulletin of the Seismological Society of America*, vol. 103, no. 1, pp. 236–246, 2013.

[35] W. Wu, S. Wang, C. Chen, and G. Lai, "Assessment of environmental and nondestructive earthquake effects on modal parameters of an office building based on long-term vibration measurements," *Smart Materials and Structures*, vol. 26, no. 5, p. 055034, 2017.

[36] S. Bennati, L. Nardini, and W. Salvatore, "Dynamic behavior of a medieval masonry bell tower. II: Measurement and modeling of the tower motion," *Journal of Structural Engineering*, vol. 131, no. 11, pp. 1656–1664, 2005.

[37] S. Ivorra and F. J. Pallares, "Dynamic investigation on a masonry bell tower," *Eng Struct*, vol. 25, no. 6, pp. 660–667, 2006.

[38] C. Gentile and A. Saisi, "Ambient vibration testing of historic masonry towers for structural identification and damage assessment," *Construction and Building Materials*, vol. 21, no. 6, pp. 1311–1321, 2007.

[39] L. F. Ramos, L. Marques, P. B. Lourenço, G. De Roeck, A. Campos-Costa, and J. Roque, "Monitoring historical masonry structures with operational modal analysis: Two case studies," *Mechanical Systems and Signal Processing*, vol. 24, no. 5, pp. 1291–1305, 2010.

[40] L. J. Sánchez-Aparicio, B. Riveiro, D. González-Aguilera, and L. F. Ramos, "The combination of geomatic approaches and operational modal analysis to improve calibration of finite element models: A case of study in Saint Torcato Church (Guimarães, Portugal)," *Construction and Building Materials*, vol. 70, pp. 118–129, 2014.

[41] A. Saisi, C. Gentile, and M. Guidobaldi, "Post-earthquake continuous dynamic monitoring of the Gabbia Tower in Mantua, Italy," *Construction and Building Materials*, vol. 81, pp. 101–112, 2015.

[42] P. Van Overschee and B. L. De Moor, *Subspace identification for linear systems*, Kluwer Academic Publishers, Leuven, Belgio, 1996.

[43] M. Döhler, E. Reynders, F. Magalhães, L. Mevel, G. D. Roeck, and Á. Cunha, "Pre- and Post-identification Merging for Multi-Setup OMA with Covariance-Driven SSI," *Dynamics of Bridges*, vol. 5, pp. 57–70, 2011.

[44] SAP2000 advanced (v14.1.0) "Static and dynamic finite element analysis of structures", Berkeley, CSI Computer & Structures, Inc., 2009.

[45] EN 1992-1-1: Design of concrete structures Part 1-1: General rules and rules for buildings,.

[46] F. D. Lydon and R. V. Balendran, "Some observations on elastic properties of plain concrete," *Cement and Concrete Research*, vol. 16, no. 3, pp. 314–324, 1986.

[47] "Advertisement - National Instruments," *IEEE Signal Processing Magazine*, vol. 24, no. 2, pp. c2–c2, 2007.

[48] W.-H. Hu, Á. Cunha, E. Caetano, F. Magalhães, and C. Moutinho, "LabVIEW toolkits for output-only modal identification and long-term dynamic structural monitoring," *Structure and Infrastructure Engineering*, vol. 6, no. 5, pp. 557–574, 2010.